International Journal of Multidisciplinary Research and Modern Education (IJMRME))
ISSN (Online): 2454 - 6119
(www.rdmodernresearch.org) Volume I, Issue I, 2015

INTELLIGENT SENSOR LESS AND ROTOR FLUX LINKAGE CONTROL DESIGN OF PERMANENT-MAGNET SYNCHRONOUS MOTORS SERVO DRIVE

S. Radhika*, Dr. R. A. Jaikumar & Dr. M. Marsalin Beno*****
*Research Scholar, St. Peter's University, Avadi, Chennai, Tamilnadu
** Formerly Principal, Athwaitha Mission Engineering College, Bhakka, Bihar
***Professor & Head, Department of Electrical & Electronics Engineering,
St. Xavier's Catholic College of Engineering, Kanyakumari, Tamilnadu

Abstract:

Due to the high power density the permanent-magnet synchronous motors (PMSM) are widely used in industrial servo applications. However, there exists a risk of potential irreversible demagnetization in the rotor magnets due to high temperature rise or large demagnetizing current. Since the rotor permanent magnet (PM) flux linkage decreases as the PM temperature increases, it is desirable to estimate the rotor flux linkage value since the decrease in rotor flux linkage in turn reduces the performance of the drive. Sensor less control method is also involved to improve the performance of machine. The proposed method consists of a thermocouple and an adaline estimator which estimates the temperature of the machine and distortion in the voltage respectively. The thermocouple is placed on either sides of the stator. By continuously monitoring or tracking the rotor flux linkage and compensating the VSI nonlinearity the performance of the PMSM can be improved. Hence the machine can possess high efficiency.

Keywords: PMSM, Fuzzy Controller, Extrusion System, Fuzzy PID, LabVIEW Program , Accelerated fuzzy PI, Intelligent Hybrid Fuzzy, Neuro Fuzzy Controller, PWM, PID Controller, Neural Controller & Synthetic Optimizing.

I. Introduction:

The permanent-magnet synchronous motors (PMSM) are widely employed in industrial servo drives, electric/hybrid electric vehicles, wind power generators etc due to its high power density. During the continuous operation of the motor the temperature of the rotor may increase in high level as it is a permanent magnet. Also there occur some problems in the permanent magnet during the time of start up, synchronization and voltage regulation. The increase in temperature of the rotor further decreases the rotor flux linkage and hence the performance of the drive may get affected. So the continuous monitoring of the rotor flux linkage is necessary to increase the performance. The magnetic materials of the permanent magnet synchronous motors are sensitive to temperature; for instance, the magnet can lose its magnetic qualities at high temperatures. Hence the rotor temperature must be supervised. It is important to obtain accurate machine parameters for online fault diagnosis and monitoring rotor/stator temperature, as well as for achieving high control performance. The rotor flux linkage can be estimated using the sensor less operation of PMSM drive because of the high cost and difficulty of installing sensors.

II. Proposed System:

A method for online estimating the PMSM rotor flux linkage and distorted voltage V dead due to VSI nonlinearity is proposed, which is suitable for most widely used id=0 control and also used for the condition monitoring of the rotor PM. The winding resistance at normal temperature and temperature coefficient of winding resistance are measured before the implementation of the proposed method. Thermocouples are employed for measuring the temperature variation in stator winding resistance, which is used for aiding the estimation of rotor flux linkage. Thus,

this method does not need to inject any signals such as id≠0 and dc voltage pulse or change the PMSM working condition. Also, it is advanced that the accuracy of the proposed rotor flux linkage estimation will not suffer from the variation of dq-axis inductances and has taken into account the compensation of estimation error due to VSI nonlinearity. This method is experimentally validated in a field oriented vector control system and shows good performance in tracking the variation of the PMSM rotor flux linkage and compensating the VSI nonlinearity. Since it is suitable for only id=0 control, the estimation for id≠0 will also being proposed.

III. Overall Block Diagram:

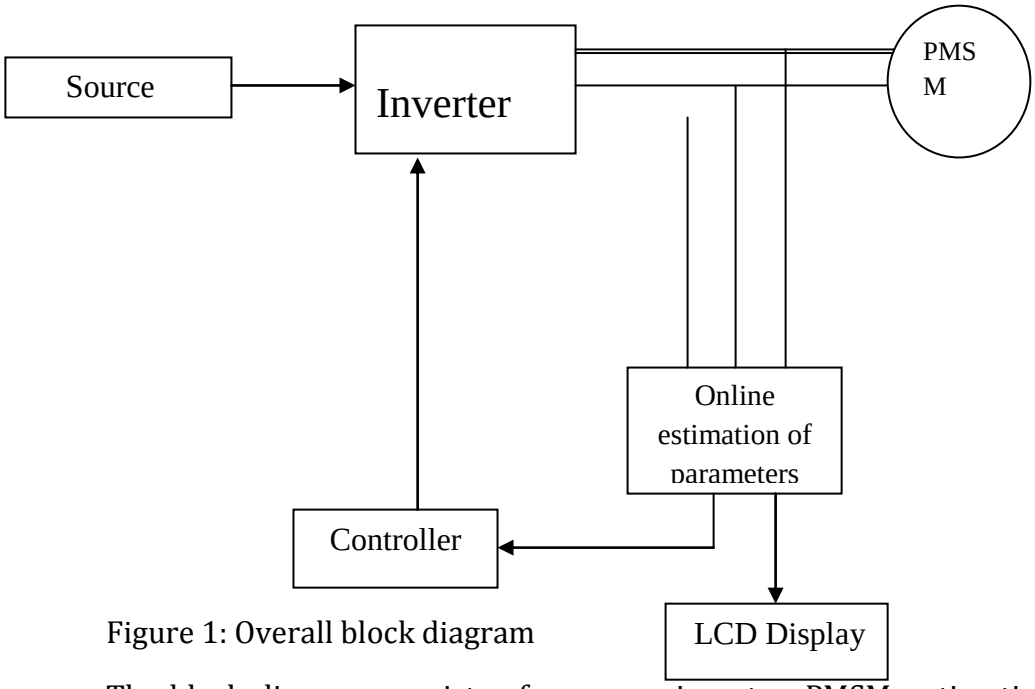

Figure 1: Overall block diagram

The block diagram consists of a source, inverter, PMSM, estimation part and a controller. The source can be a dc source which is fed to the inverter and the inverter uses the space vector pulse width modulation to convert the dc source to ac supply for the motor. The online estimation of parameters is based on the simple fact that the rate of change of flux will produce emf in the circuit. This can be given by

$$v \propto \frac{d\phi}{dt}$$

IV. Sensor less Control of PMSM:

The sensor less control of the permanent magnet synchronous motor is used to determine the angular velocity without using any sensors.

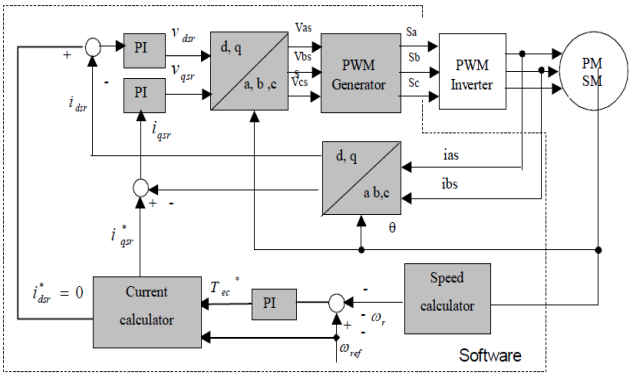

Figure 2: Sensor less control of permanent magnet synchronous motor.

The rotor speed of the PMSM can be fed to the speed calculator from which the actual speed is generated. Then the actual speed and the reference speed can be compared using the comparator and the error is cleared using the PI controller. The three phase components of the current from the PMSM are converted into two phase components by using park's transformation. The d-axis component of the current is made zero in order to improve the performance and accuracy. The dq-axis currents are converted into respective voltages and again the dq-axis voltages are converted into three phase voltages (va, vb, vc) which are used for the generation of PWM pulses to the inverter. The supply for the PMSM is fed by the three phase inverter.

V. Online Estimation of Rotor Flux Linkage:

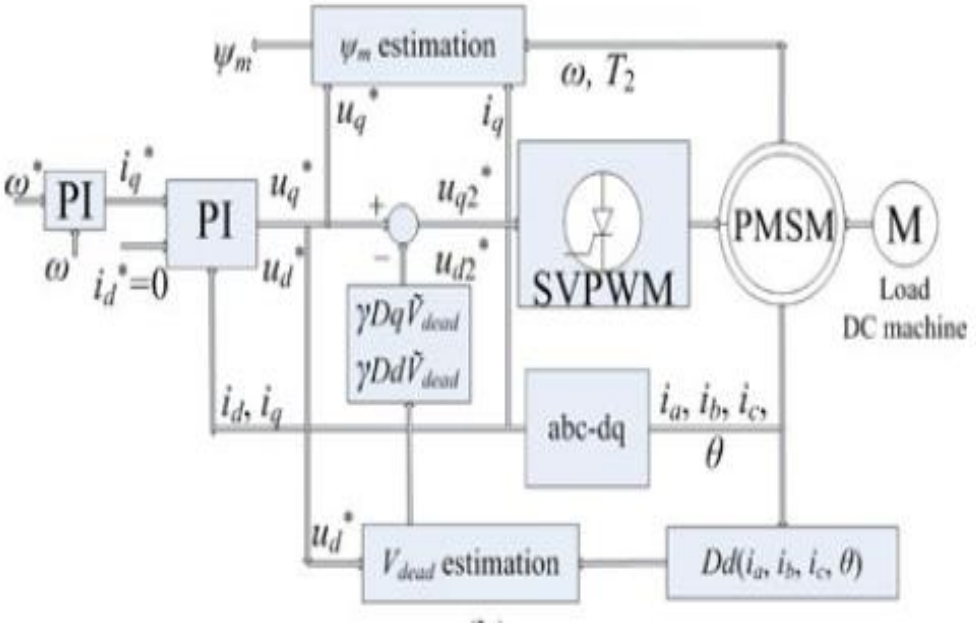

Figure 3 Process of online estimation of rotor flux linkage and compensating VSI non linearity

Mathematical model for the estimation of rotor flux linkage and distortion in the voltage of the voltage source inverter can be given by,

The dq-axis equations of the PMSM are,

$$\frac{did}{dt} = -\frac{R}{Ld}id + \frac{Lq}{Ld}\omega iq + \frac{vd}{Ld}$$

$$\frac{diq}{dt} = -\frac{R}{Lq}iq - \frac{Ld}{Lq}\omega id + \frac{vq}{Lq} - \frac{\psi m}{Lq}\omega$$

The steady-state dq-axis equations of the PMSM are,

$$vd(k) = Rid(k) - Lq\omega(k)iq(k)$$

$$vq(k) = Riq(k) + Ld\omega(k)id(k) + \psi m\omega(k)$$

Where,

k→ Index of the discrete sampling instant.

When id=0, the equations can be simplified into,

$$vd(k) = -Lq\omega(k)iq(k)$$

$$vq(k) = Riq(k) + \psi m\omega(k)$$

The dq-axis equations including voltage distortion due to VSI non-linearity is given by,

$$\frac{d}{dt}\begin{matrix}Ldid\\Lqiq\end{matrix}=-R\begin{matrix}id\\iq\end{matrix}+\begin{matrix}Lq\omega iq\\-Ld\omega id-\psi m\omega\end{matrix}+\begin{matrix}vd*\\vq*\end{matrix}+Vdead\begin{matrix}Dd\\Dq\end{matrix}$$

Where Dd and Dq are expressed as,

$$\begin{matrix}Dd\\Dq\end{matrix}=2\begin{matrix}\cos\theta & \cos(\theta-\frac{2\pi}{3}) & \cos(\theta+\frac{2\pi}{3})\\-\sin\theta & -\sin(\theta-\frac{2\pi}{3}) & \sin(\theta+\frac{2\pi}{3})\end{matrix}\begin{matrix}sign(ias)\\sign(ibs)\\sign(ics)\end{matrix}$$

sign (i) = $\begin{cases}1, i>=0\\-1, i<0.\end{cases}$

Using dq-axis steady state equations of the PMSM, the rotor flux linkage equation can be estimated as,

$$Lq\frac{diq}{dt}=vq-Rqiq+\omega Ldid-\Psi m\omega$$

$$\Psi m\omega=Lq\frac{diq}{dt}-vq+Rqiq-\omega Ldid$$

$$\psi m=\frac{Lq}{\omega}\frac{diq}{dt}-\frac{vq}{\omega}+\frac{Rqiq}{\omega}-Ldid$$

The VSI nonlinearity in the system can be measured using,

$$vd+DdVdead=Rid-Lq\omega iq$$

$$DdVdead=Rid-Lq\omega iq-vd$$

$$Vdead=\frac{Rid}{Dd}-\frac{Lqiq\omega}{Dd}-\frac{vd}{\omega}$$

Actual value of winding resistance can be measured using,

R=Ro+ TCR(T2-To) →(A)

Where,

Ro→ Winding resistance at room Temperature (To=27degree)

TCR→ Temperature Coefficient.

T2→ Increase in temperature during Running.

VI. Compensation of VSI Non Linearity:

With aiding from the estimated *V* dead and computed winding resistance *R*, the rotor flux linkage can be finally estimated by (A). The complete diagram of the proposed method is shown in Fig. 4 and the whole estimation are divided into three steps:

1) At standstill, the stator winding resistance value *R*0 at normal temperature *T*0 is measured by milliohm meter and two sets of thermocouple are employed for measuring the variation of stator winding temperature *T*2, which will be used for real time computing the actual value of stator winding resistance *R*.

2) The value of *V* dead of distorted voltage due to VSI nonlinearity is online estimated from the *d*-axis equation and employed for the compensation of inverter nonlinearity.

3) The rotor flux linkage is finally estimated from the *q*-axis equation with the aiding from computed winding resistance and *V* dead.

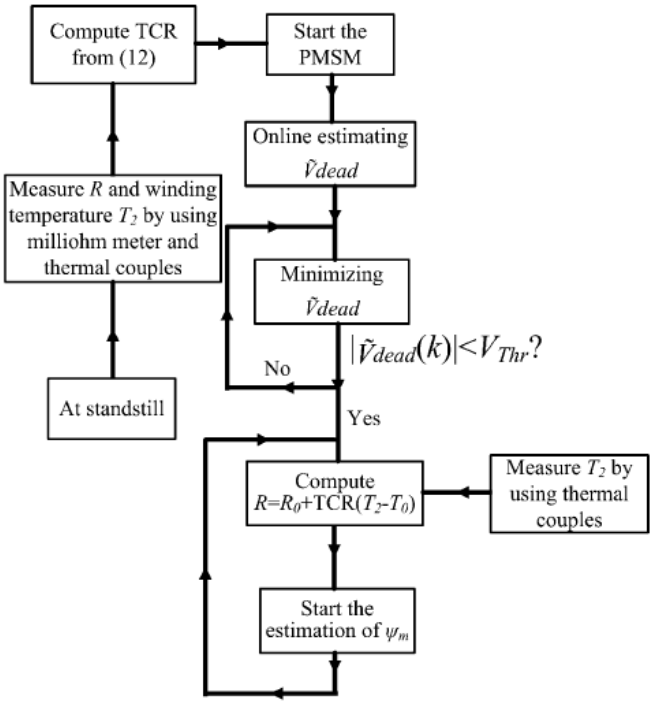

Figure 4: Flowchart for the estimation of rotor flux linkage.

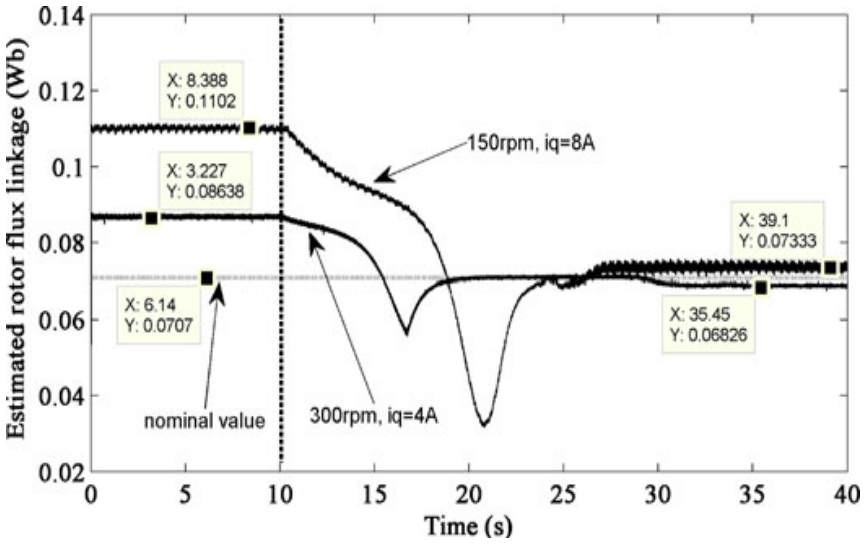

Figure 5: Estimated rotor flux linkage with and without compensation at normal temperature.

The estimation of the rotor flux linkage under different working conditions is depicted in Fig. 5, in which the estimation and compensation of *V*dead are started after *t* = 10 s. From Fig. 5, it is obvious that the estimated rotor flux linkage at 300 r/min (68.3 mWb) is close to that under no-load condition (70.7 mWb) and the slight decrease in the rotor flux linkage (70.7–68.3 = 2.4 mWb) can be explained that it is caused by the variation of flux density due to on load. However, the estimated rotor flux linkage at 150 r/min (73.3 mWb) is slightly larger than that under no-load condition (70.7 mWb), which is contrary to the basic theory that the rotor flux linkage under loaded condition should be smaller than that under no-load condition. This estimation error can be

explained that there are still influences from other nonlinearities such as non ideal position measurement, current offsets, and non ideal measurement of dc-bus voltage.

VII. Permanent Magnet Synchronous Motor:

A permanent magnet synchronous motor is a motor where the excitation field is provided by a permanent magnet instead of a coil. Synchronous generators are the majority source of commercial electrical energy. They are commonly used to convert the mechanical power output of steam turbines, gas turbines, reciprocating engines, hydro turbines and wind turbines into electrical power for the grid. In the majority of designs the rotating assembly in the center of the generator the "rotor" contains the magnet, and the "stator" is the stationary armature that is electrically connected to a load. A set of three conductors make up the armature winding in standard utility equipment, constituting three phases of a power circuit that correspond to the three wires we are accustomed to see on transmission lines.If the rotor windings are arranged in such a way as to produce the effect of more than two magnetic poles, then each physical revolution of the rotor results in more magnetic poles moving past the armature windings. Each passing of a north and South Pole corresponds to a complete "cycle" of a magnet field oscillation. Therefore, the constant of proportionality is

$$\frac{\mathrm{P}}{120},$$

Where P is the number of magnetic rotor poles (almost always an even number), and the factor of 120 comes from 60 seconds per minute and two poles in a single magnet;

$$f\,(\mathrm{Hz}) = RPM\frac{\mathrm{P}}{120.}$$

In a permanent magnet generator, the magnetic field of the rotor is produced by permanent magnets. Other types of generator use electromagnets to produce a magnetic field in a rotor winding. The direct current in the rotor field winding is fed through a slip-ring assembly or provided by a brushless exciter on the same shaft. Synchronous motors fall under the more general category of synchronous machines which also includes the synchronous generator. Generator action will be observed if the field poles are "driven ahead of the resultant air-gap flux by the forward motion of the prime mover". Motor action will be observed if the field poles are "dragged behind the resultant air-gap flux by the retarding torque of a shaft load". There are two major types of synchronous motors depending on how the rotor is magnetized: non-excited and direct-current excited.

a. Construction:

Figure 6: Rotor of a large water pump. The slip rings can be seen below the rotor drum.

Figure 7: Stator winding of a large water pump

The principal components of a synchronous motor are the stator and the rotor. The stator of synchronous motor and stator of induction motor are similar in construction. The stator frame contains wrapper plate. Circumferential ribs and key bars are attached to the wrapper plate. To carry the weight of the machine, frame mounts and footings are required. When the field winding is excited by DC excitation, brushes and slip rings are required to connect to the excitation supply. The field winding can also be excited by a brushless exciter. Cylindrical, round rotors, (also known as non salient pole rotor) are used for up to six poles. In some machines or when a large number of poles are needed, a salient pole rotor is used. The construction of synchronous motor is similar to that of a synchronous alternator.

b. Starting Methods:

Above a certain size, synchronous motors are not self-starting motors. This property is due to the inertia of the rotor; it cannot instantly follow the rotation of the magnetic field of the stator. Since a synchronous motor produces no inherent average torque at standstill, it cannot accelerate to synchronous speed without some supplemental mechanism. Large motors operating on commercial power frequency include a "squirrel cage" induction winding which provides sufficient torque for acceleration and which also serves to damp oscillations in motor speed in operation. Small synchronous motors are commonly used in line-powered electric mechanical clocks or timers that use the power line frequency to run the gear mechanism at the correct speed. Synchronous motors in clocks typically use an anti-reversing mechanism to ensure starting in the correct direction.

c. Use as Synchronous Condenser:

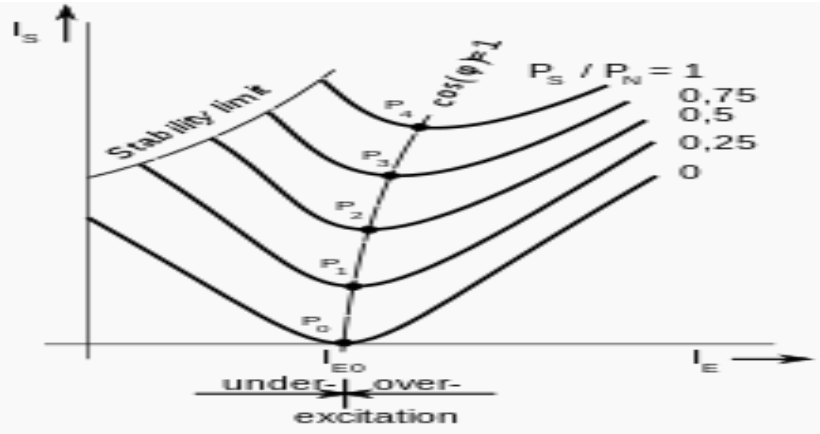

Figure 8: V-curve of a synchronous machine

By varying the excitation of a synchronous motor, it can be made to operate at lagging, leading and unity power factor. Excitation at which the power factor is unity is termed normal excitation voltage. When the motor is over excited, the back emf will be greater than the motor terminal voltage. This causes a demagnetizing effect due to armature reaction. This ability to selectively control power factor can be exploited for power factor correction of the power system to which the motor is connected. Since most power systems of any significant size have a net lagging power factor, the presence of overexcited synchronous motors moves the system's net power factor closer to unity, improving efficiency. Such power-factor correction is usually a side effect of motors already present in the system to provide mechanical work, although motors can be run without mechanical load simply to provide power-factor correction. In large industrial plants such as factories the interaction between synchronous motors and other, lagging, loads may be an explicit consideration in the plant's electrical design.

Steady state stability limit

$$\mathbf{T} = \mathbf{T_{max}} \sin \delta$$

Where,

$\mathbf{T}$ is the torque

δ is the torque angle

$\mathbf{T_{max}}$ is the maximum torque

Here,

$$\mathbf{T_{max}} = \frac{\mathbf{3VE}}{\mathbf{X_s}\omega_s}$$

When load is applied, torque angle δ increases. When δ = 90° the torque will be maximum. If load is applied further then the motor will lose its synchronism, since motor torque will be less than load torque. The maximum load torque that can be applied to a motor without losing its synchronism is called steady state stability limit of a synchronous motor.

VIII. Mathematical Model of PMSM:

The following assumptions are made before establishing the mathematical model of PMSM:

- Neglects the saturation of the electric motor ferrite core.
- Neglects turbulent flow and hysteresis loss in electric motor.
- The current in electric motor is symmetrical three phase sinusoidal current.

a. d-q Reference Coordinate System:

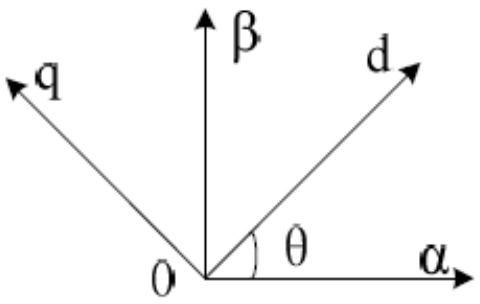

Figure 9: Relationship of α-β coordinate system and d-q coordinate system.

The most common method in analyzing electric control PMSM is d-q axis mathematical model, which can be used in analyzing the stable state performance of PMSM as well as in studying the transient state performance. The mathematical model

of PMSM is usually composed of the voltage equation, the stator flux linkage equation, the electromagnetism torque equation, the mechanical movement equation. The equations under d-q coordinate system can be expressed as follows:

The stator voltage equations are

$$Vq = RsIq + p\lambda q + \omega\lambda d \qquad (1)$$
$$Vd = RsId + p\lambda d - \omega\lambda q$$

Flux linkages in the coils are

$$\lambda_q = LqIq^s + LmIq^r \qquad (2)$$

Assuming

$$\lambda_d = LdId^s + LmId^r$$

Equation (2) becomes

$$Id^r = if\,,\ Iq^r = 0 \qquad (3)$$
$$\lambda_q = LqIq^s$$
$$\lambda_d = LdId^s + Lmif$$

Substituting this in voltage equation (1)

$$Vq = RsIq + p\lambda_q + \omega LdId + \omega Lmif \qquad (4)$$
$$Vd = RsId + p\lambda_d - \omega LqIq$$

Electromagnetic torque equation is

$$Te = p(Iq\lambda d - Id\lambda q) \qquad (5)$$

Mechanical movement equation is

$$\frac{J}{p}\frac{d\omega}{dt} = Te - Tl \qquad (6)$$

Where:

Vd,Vq	-Applied d-q-axis control voltage
Id,Iq	-Stator d-q-axis current
λd,λq	-d-q-axis flux linkage
Ld,Lq	-d-q-axis inductance
Rs	-Armature resistance
P	-Pole-pair numbers of the motor
ω	-Electrical angular speed

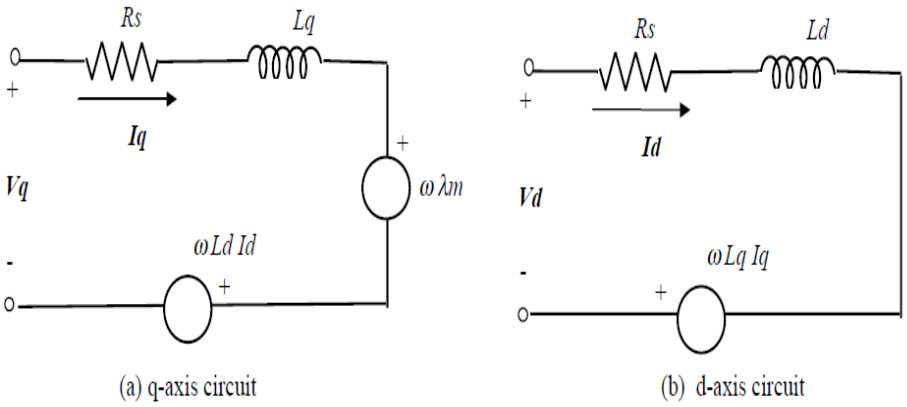

Figure 10: Equivalent circuit

IX. Space Vector Pulse Width Modulation:

a. Space vector modulation:

Space vector modulation (**SVM**) is an algorithm for the control of pulse width modulation (PWM). It is used for the creation of alternating current (AC) waveforms; most commonly to drive 3 phase AC powered motors at varying speeds from DC using multiple class-D amplifiers. There are various variations of SVM that result in different quality and computational requirements. One active area of development is in the reduction of total harmonic distortion (THD) created by the rapid switching inherent to these algorithms.

b. Principle:

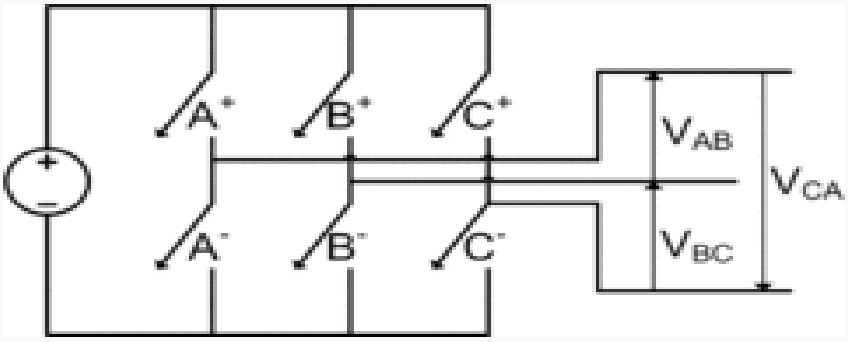

Figure 11: Topology of a basic three phase inverter.

A three phase inverter as shown to the right must be controlled so that at no time are both switches in the same leg turned on or else the DC supply would be shorted. This requirement may be met by the complementary operation of the switches within a leg. i.e. if A^+ is on then A^- is off and vice versa. This leads to eight possible switching vectors for the inverter, V_0 through V_7 with six active switching vectors and two zero vectors. To implement space vector modulation a reference signal V_{ref} is sampled with a frequency f_s ($T_s = 1/f_s$). The reference signal may be generated from three separate phase references using the $\alpha\beta\gamma$ transform.

The reference vector is then synthesized using a combination of the two adjacent active switching vectors and one or both of the zero vectors. Various strategies of selecting the order of the vectors and which zero vector(s) to use exist. Strategy selection will affect the harmonic content and the switching losses. More complicated SVM strategies for the unbalanced operation of four-leg three-phase inverters do exist.In these strategies the switching vectors define a 3D shape (a) hexagonal prism in $\alpha\beta\gamma$coordinates or a dodecahedron in abc Three-Dimensional Space Vector Modulation in abc coordinates) rather than a 2D hexagon.

c. Space Vector Pulse Width Modulation Technique:

In motor theory, motor speed is defined by the formula

$$N=\frac{60f}{p} \qquad (7)$$

Where f-Power frequency and p-pole pair

Through the formula ,speed regulate need change the power frequency or the motor pole pairs, and change power frequency easier than change motor pole pairs, so, at present, the great mass of motor speed regulate use frequency convert. Currently, use the type of: AC-DC-AC. It's means, convert 3-phase power AC into DC, then, invert the DC into 3-phase AC and change frequency. First, define the 3-phase power AC interphase voltage is:

$$Ua = \sqrt{2}\,U(cos\omega t)$$
$$Ub = \sqrt{2}\,Ucos(\omega t - \frac{2\pi}{3}) \quad (8)$$
$$Uc = \sqrt{2}Ucos(\omega t - \frac{4\pi}{3})$$

Convert this 3-phase AC voltage into stationary system (α-β):

$$U_\alpha = 2/3(Ua - 0.5Ub - 0.5Uc = \sqrt{2}U\ (cos\omega t)$$
$$U_\beta = -2/3(\sqrt{\frac{3}{2}}\,Ub - \sqrt{\frac{3}{2}}\,Uc = \sqrt{2}\mathrm{U}(\sin\omega t) \quad (9)$$

Take this into voltage space vector:

$$Us = U\alpha + jU\beta$$
$$Us = \sqrt{2}(\cos\omega t + j\sin\omega t) = \sqrt{2}Ue^{j\omega t} \quad (10)$$

This equation is circular in plural plane. So, in motor theory, invariableness' voltage (U) and frequency, stator voltage space vector in plural plane move along with a circularity , and space vector move a cycle in a power frequency cycle. After Clark transforming, phase voltage in the three-phase ABC plane coordinate system can be change into αβ right-angled coordinate system.

d. DC-AC Converter:

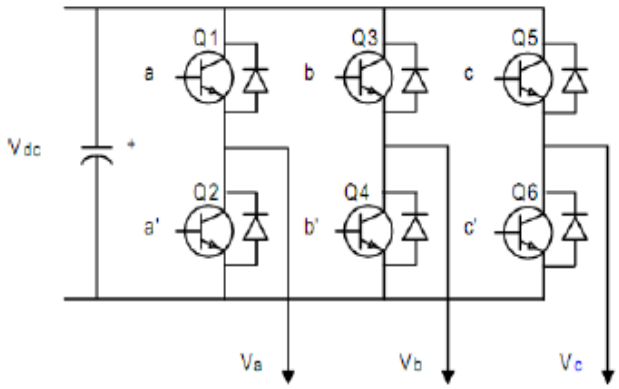

Figure 12: dc to ac converter

It has six power switches a, b, c, a', b', c' which are grouped into S(a, b, c) and S(a', b', c').It means each voltage vector is coded by three digit number and have eight possible switching states.

Consider the state S(1,0,0).

The point [a], [b'], [c'] switch ON, and [a], [b], [c] switch OFF.

Uan=Udc and Ubn=Ucn=0

Substitute these values in (3.5)

$$Ua = \frac{2Udc}{3}\ Ub = -\frac{Udc}{3}\quad Uc = -\frac{Udc}{3} \quad (11)$$

Graphical representation of all combinations is the hexagon shown in Figure 13. There are six non-zero vectors, U0, U60, U120, U180, U240, U300, and two zero vectors, O000 and O111 defined in α, β coordinates.

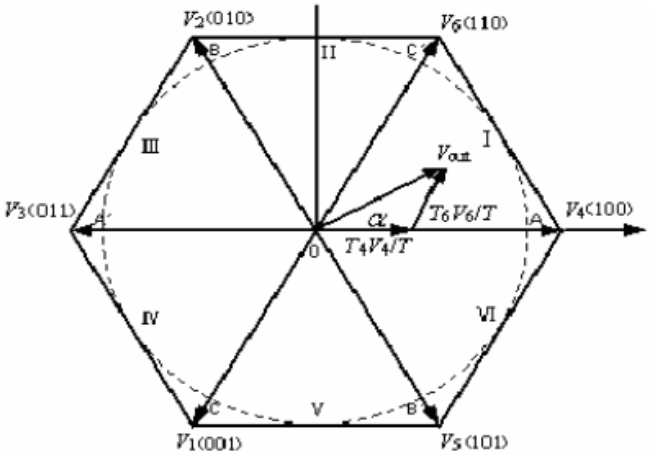

Figure 13: Vector Representation

e. Procedure for SVPWM Production:

1. Make sure the Uref belong to which sector.
2. Calculate X, Y, Z which is used to determine open time of 2 adjacent basic vectors.
3. Determine each conduction time t1,t2 for 2 adjacent basic vector.
4. Calculate taon, tbon, tcon which are used to create SVPWM waveform.

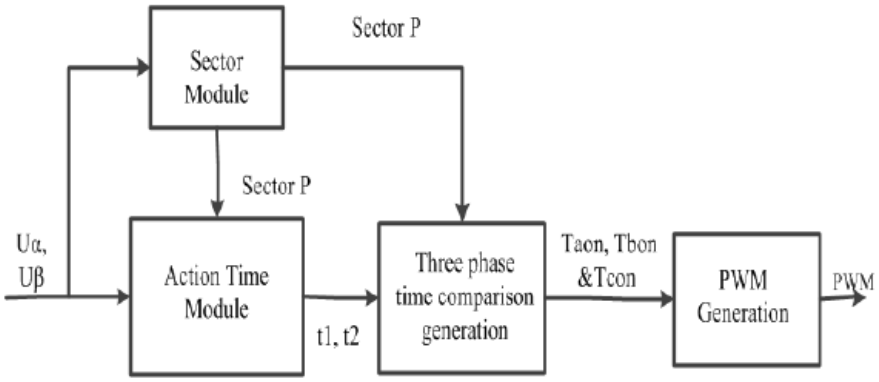

Figure 14: Block diagram of SVPWM

f. Judgement Sector:

According to figure 14, when *V*out is given in the form of the component *V*outα、*V*outβ on *α*-*β* coordinate system, we can use equation (8) to calculate *B*0,*B*1,*B*2.

B0= Uβ

B1=sin 60 Uα –sin 30 Uβ

B2= -sin 60 Uα –sin 30 Uβ (12)

The value of equation P can be written as

P=4sign(B2)+2sign(B1)+sign(B0) (13)

where sign(x) is sign function.

Then the sector number can be given by

Table 1: Sector Number

P	1	2	3	4	5	6
Sector number	2	6	1	4	3	5

g. Act time of basic voltage vector

The relationship between the act time of the basic voltage vectors $t1$、$t2$ and X、Y、Z, and sector N is shown as follows:

Table 2: Act Time of Voltage Vector

Sector N	1	2	3	4	5	6
t1	Z	Y	-Z	-X	X	-Y
t2	Y	-X	X	Z	-Y	-Z

Where

$$X=\sqrt{3}V\alpha Ts/Udc$$
$$Y=0.5(\sqrt{3}V\beta+3V\alpha)Ts/Udc \quad (14)$$
$$Z=0.5(\sqrt{3}V\beta-3V\alpha)Ts/Udc$$

h. Calculation of switching time

Firstly, Ta,Tb,Tc can be given by

$$Ta=\frac{T-T1-T2}{2} \qquad Tb=\frac{Ta+T1}{2} \qquad Tc=\frac{Tb+T1}{2} \quad (15)$$

The switch time is shown as in the following table, where taon, tbon, tcon means the turned-on time of the three-phase bridge arm power component respectively.

X. Result and Analysis:

a. Simulink model for online estimation and sensor less control of PMSM:

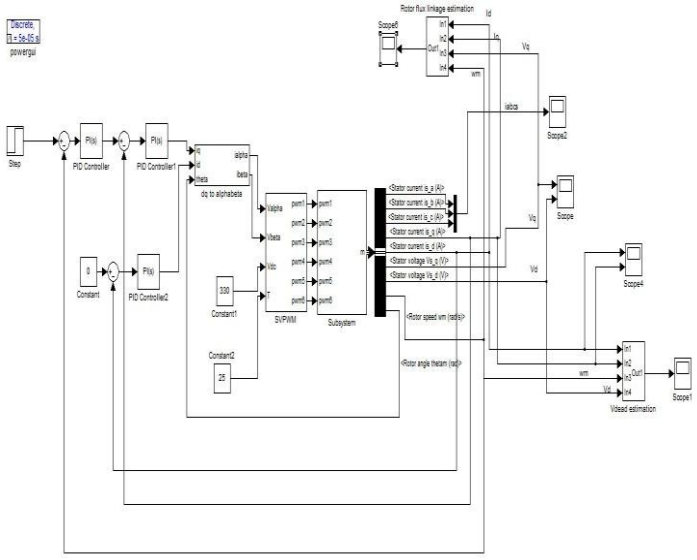

Figure 15: Simulation block diagram of online estimation of rotor flux linkage and sensor less control of PMSM

Figure 15 shows the simulation diagram for the online estimation of rotor flux linkage and distortion in the voltage. The system includes the PI controller for the speed loop and the inner current loop. dq/αβ block, SVPWM, VSI block with IGBT and a PMSM model. The selected PI values of the outer speed loop are P equal to 0.01 and I equal to 4. The PI parameters of inner current loop are P=4 and I=0.11. The controllers are tuned according to trial and error method. The direct voltage bus is 300v. The switching frequency is taken as 10 KHz and a PWM carrier frequency is of 5 KHz. Simulation is carried out for 0.1 sec. The PMSM control system mainly includes: PMSM power module, coordinate transformation module and SVPWM production module. The online estimation of parameters includes: rotor flux linkage estimation and V dead estimation.

b. Coordinate Transformation Module:

The transformation module transforms the currents in d-q reference frame to the alpha beta frame. Fig 16 shows the transformation module.

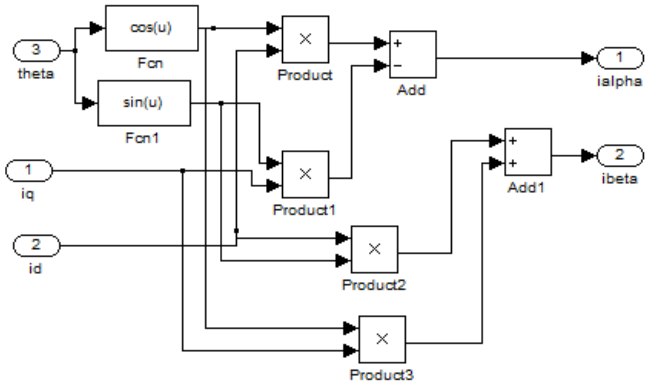

Figure 16: transformation module

c. SVPWM Module:

The SVPWM module includes sector judgement module, calculation of X,Y,Z for the act time basic voltage vector , calculation of switching time taon,tbon,tcon. Figure 17 shows the calculation of X,Y,Z .

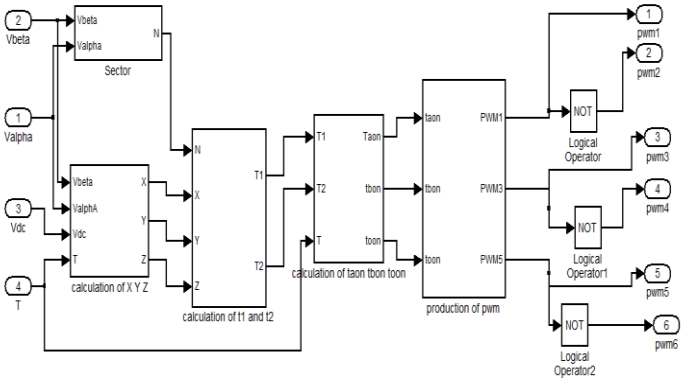

Figure 17: SVPWM module

d. Sector Judgement Module:

This module determines the sector in which the voltage vector is present. Fig 18 shows the sector judgement module.

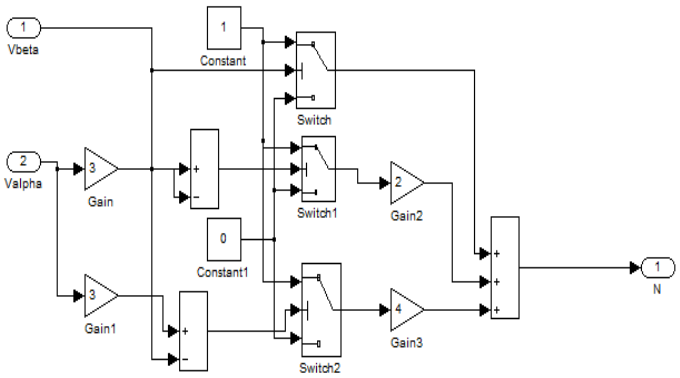

Figure 18: sector judgement module

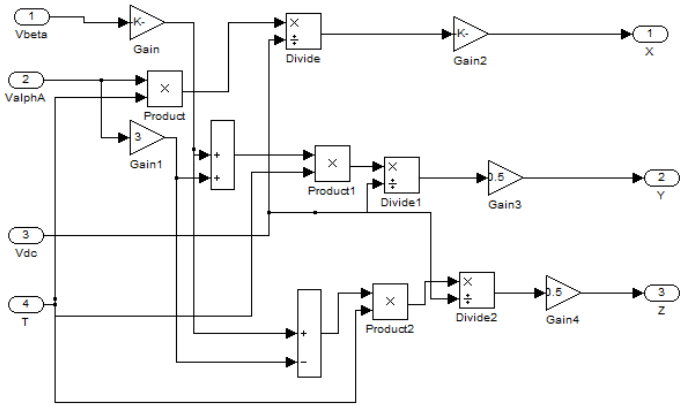

Figure 19: Calculation of X, Y, Z4.

e. Act time of Basic Voltage Vector:

Figure 20 shows the calculation of X,Y,Z and Fig 20 shows the calculation of t1 ,t2 .

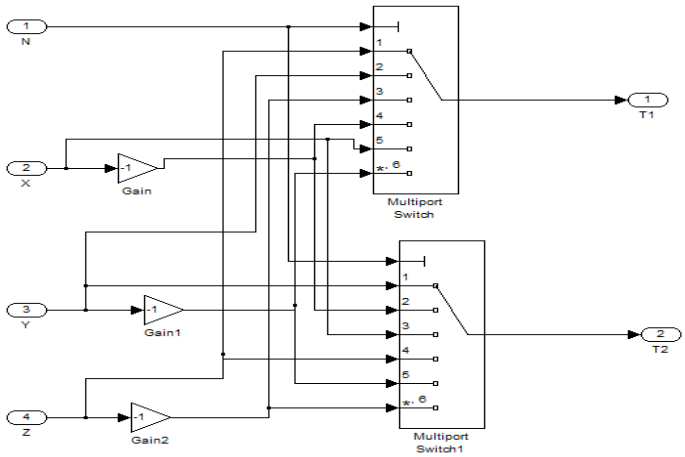

Figure 20: Calculation of t1, t2

f. Inverter Switching Time:

The switching time of three phases taon, tbon, tcon are calculated. These values are required to generate the PWM signals for the inverter. Fig 21 shows the calculation of switching time of inverter

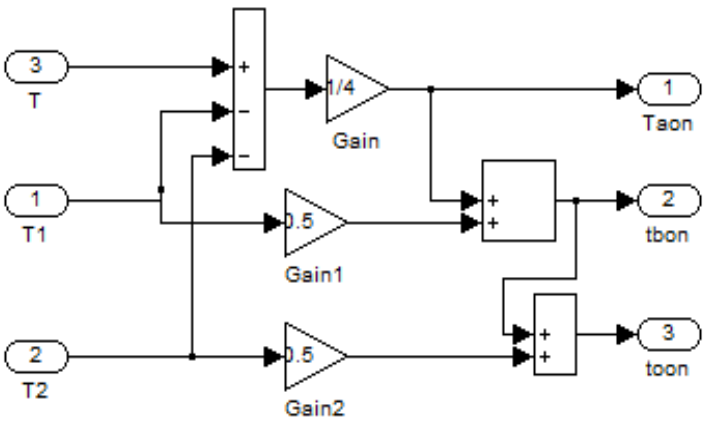

Figure 21: Switching Time Calculation

g. Power Module:

The power module contains the three phase inverter and the synchronous machine. Fig 22 shows the power module. The load torque is set at 1Nm.The direct bus voltage is given as 300V.

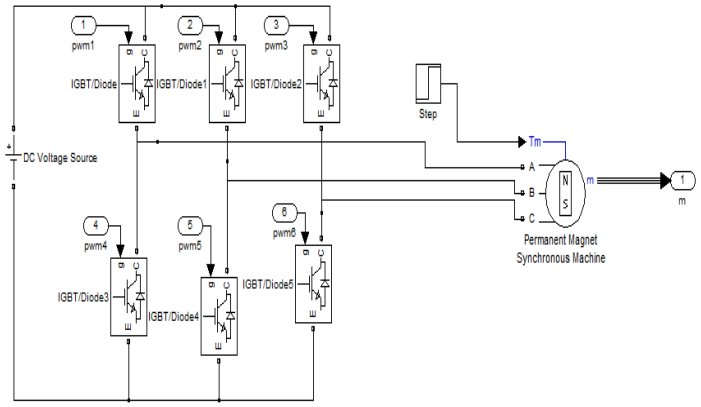

Figure 22: Power Module

The measurement module may be used for examining the outputs physical quantity of the motor, and as feedback parameter to constitute closed-loop control system.

h. Rotor Flux Linkage Estimation:

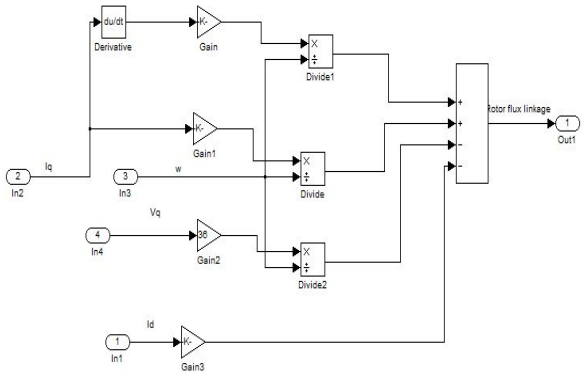

Figure 23: Rotor flux linkage estimation

The rotor flux linkage of the PMSM can be estimated using the figure 23.

i. Vdead Estimation:

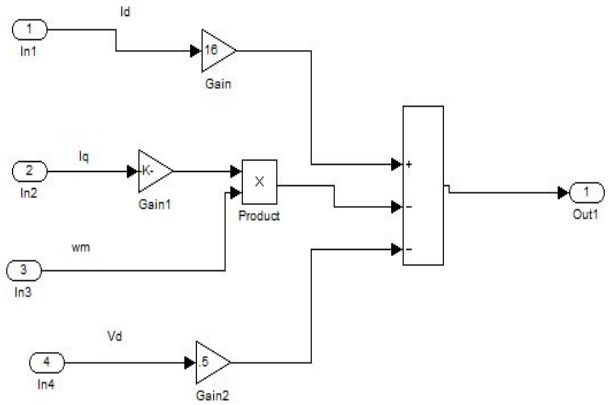

Figure 24: Voltage distortion estimation

Figure 24 shows the calculation of the distorted voltage of the PMSM.

The response of the estimated rotor flux linkage and VSI nonlinearity Vdead can be given by,

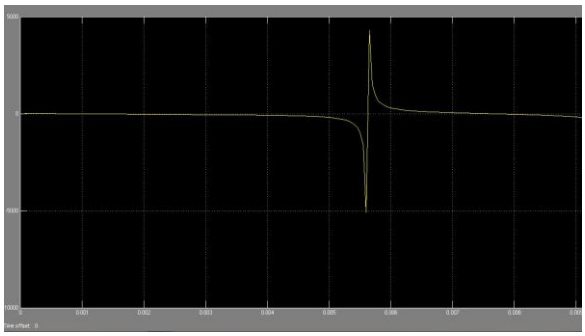

Figure 25 Response of rotor flux linkage. The rotor flux linkage of the PMSM can be found to be settled at 70.7mWb.

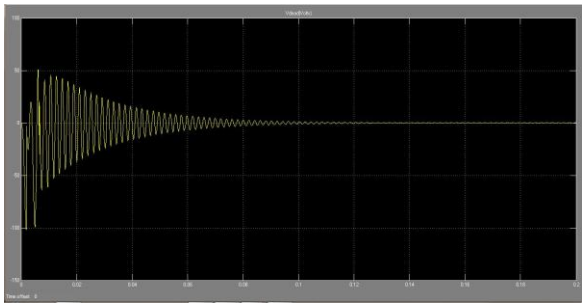

Figure 26 response of voltage distortion.

XI. Conclusion:

The Sensorless and Rotor Flux Linkage Control Design of PMSM is used for the sensor less field oriented control of PMSM using MATLAB/SIMULINK. The results of simulations indicate that the system gives desired response. Therefore the SVPWM model is an effective tool for studying sinusoidal back emf motor drive systems. The complex trigonometric calculations in the conventional SVPWM technique is converted to simple addition and subtraction logics, by using intermediate variable and orthogonal decomposition of reference vector. A new scheme for the online estimation of PMSM rotor flux linkage and VSI non linearity has been proposed which can be used for the condition monitoring of the rotor permanent magnet. By this method it is possible to improve the accuracy, performance and efficiency of the Sensorless and Rotor Flux Linkage Control Design of PMSM Servo drive.

XII. References:

1. M. N.Uddin and M. M. I. Chy, "Online parameter-estimation-based speed control of PM AC motor drive in flux-weakening region," IEEE Trans. Ind. Appl., vol. 44, no. 5, pp. 1486–1494, Sep./Oct. 2010.
2. K. W. Lee, D. H. Jung, and I. J. Ha, "An online identification method for both stator resistance and back-EMF coefficient of PMSMs without rotational transducers," IEEE Trans. Ind. Electron., vol. 51, no. 2, pp. 507–510, Apr. 2004.
3. Z. Q. Zhu, X. Zhu, and P. D. Sun, "Estimation of winding resistance and PM flux-linkage in brushless AC machines by reduced-order extended Kalman Filter," in *Proc.* IEEE Int. Conf. Netw., Sensing Control, 2007, pp. 740–745.
4. S. B. Lee, "Closed-loop estimation of permanent magnet synchronous motor parameters by PI controller gain tuning," IEEE Trans. Energy Convers., vol. 21, no. 4, pp. 863–870, Dec. 2006.

5. Piippo, M. Hinkkanen, and J. Luomi, "Adaptation of motor parameters in sensorless PMSM drives," IEEE Trans. Ind. Appl., vol. 45, no. 1, pp. 203–212, Jan./Feb. 2009.
6. S. Morimoto, M. Sanada, and Y. Yakeda, "Mechanical sensorless drives of IPMSM with online parameter identification," IEEE Trans. Ind. Appl., vol. 42, no. 5, pp. 1241–1248, Sept./Oct. 2006.
7. R. Ramakrishnan, R. Islam, M. Islam, and T. Sebastian, "Real time estimation of parameters for controlling and monitoring," in *Proc.* IEEE Int. Elect. Mach. Drives Conf., Miami, FL, USA, 2009, pp. 1194–1199.
8. P. J. Zhang, B. Lu, and T. G. Habetler, "A remote and sensorless stator winding resistance estimation method for thermal protection of soft-starter-connected induction machines," IEEE Trans. Ind. Electron., vol. 55, no. 10, pp. 3611–3618, Oct. 2008.
9. S. B. Lee and T. G. Habetler, "An online stator winding resistance estimation technique for temperature monitoring of line-connected induction machines," *I*EEE Trans. Ind. Appl., vol. 39, no. 3, pp. 685–694, Mar. 2003.
10. S. B. Lee and T. G. Habetler, "A remote and sensorless thermal protection scheme for small line-connected ac machines," IEEE Trans. Ind. Appl., vol. 39, no. 5, pp. 1323–1332, Sep./Oct. 2008.
11. S. D. Wilson, P. G. Stewart, and B. P. Taylor, "Methods of resistance estimation in permanent magnet synchronous motors for real-time thermal management," IEEE Trans. Energy Convers., vol. 25, no. 3, pp. 698–707, Sep./Oct. 2008.
12. S. D. Wilson, G. W. Jewell, and P. G. Stewart, "Resistance estimation for temperature determination in PMSMs through signal injection," in Proc. IEEE Int. Elect. Mach. Drives Conf., San Antonio, TX, USA, 2005, pp. 735–740.
13. Radhika. S, Marsalin Beno. M, Jaikumar. R.A ,"Intelligent Control Design of PMSM Servo Drive" in "National Journal on Computing and Management" Volume 4, Issue No.1, pp.32-40 April 2013.